Photochemical & Photobiological Sciences

RSC Publishing

PAPER

Photochemical properties of multi-azobenzene compounds†

Cite this: *Photochem. Photobiol. Sci.*, 2013, **12**, 511

Julia Bahrenburg,[a] Claudia M. Sievers,[a] Jan Boyke Schönborn,[a] Bernd Hartke,[a] Falk Renth,*[a] Friedrich Temps,*[a] Christian Näther[b] and Frank D. Sönnichsen*[c]

Received 22nd August 2012,
Accepted 24th November 2012

DOI: 10.1039/c2pp25291k

www.rsc.org/pps

A systematic study is reported of the photochemical properties of the multi-azobenzene compounds bis-[4-(phenylazo)phenyl]amine (BPAPA) and tris[4-(phenylazo)phenyl]amine (TPAPA) compared to the parent molecule 4-aminoazobenzene (AAB). The bis- and tris-azobenzenes were synthesised by a variant of the Ullmann reaction and exist in their stable all-*E* forms at room temperature. Striking changes in the spectral positions and intensities of their first $\pi\pi^*$ absorption bands compared to AAB reveal strong electronic coupling between the AB units. The nature of the excited states was explored by quantum chemical calculations at the approximate coupled-cluster (CC2) level. Upon UV/VIS irradiation, the molecules isomerise to the *Z*-isomer (AAB), *ZE*- and *ZZ*-isomers (BPAPA), and *ZEE*-, *ZZE*- and *ZZZ*-isomers (TPAPA), respectively. The photoswitching behaviours were investigated by UV/VIS and NMR spectroscopies. All individual isomers were detected by one-dimensional (1D) ^{1}H NMR spectroscopy (BPAPA) and two-dimensional (2D) HSQC NMR spectroscopy (TPAPA). A kinetic analysis provided the isomer-specific thermal lifetimes. The variance of the thermal lifetimes demonstrates a dependence of the *Z*–*E* isomerisation on the chromophore size and number of AB units.

1. Introduction

The reversible $E \rightleftarrows Z$ photoisomerisation of azobenzene (AB) and its derivatives upon irradiation with visible (VIS) or ultraviolet (UV) light forms the basis for a wide range of applications as light-triggered molecular switches or optical memory devices.[1–6] The high application potential of AB as a photoswitchable element rests on the reversible, large changes in size, shape and dipole moment between the thermodynamically favoured, stretched *E*-isomer and the energetically higher, more compact *Z*-isomer and on the low photochemical fatigue of the chromophore. These properties have been exploited for, *e.g.*, single molecule optomechanical research,[7,8] photoregulation of biomolecules,[9–12] photoswitching of magnetic bistability,[13] and photocontrol of macromolecular and supramolecular systems, including dendrons and dendrimers,[14–19] molecular wires[20,21] and helices,[22,23] emulsions,[24] and polymer films and materials,[25–28] which are suitable for surface patterning[29–31] or holographic information storage.[32,33] To reach the ambitious design goals for functional AB devices, however, it is mandatory to acquire detailed knowledge about the ensuing molecular dynamics under different circumstances.

In functional systems, photochromic molecular switches are typically embedded in complex environments, where the close proximity of the chromophores leads to cooperative phenomena, *e.g.*, steric interactions, excitonic coupling, charge-transfer (CT), or direct electronic coupling in π-conjugated systems. All of these mechanisms may compete with the desired photoisomerisation. To elucidate the ensuing influences, we initiated an investigation of two prototypical photoswitchable multi-azobenzene compounds, bis[4-(phenylazo)-phenyl]amine (BPAPA) and tris[4-(phenylazo)phenyl]amine (TPAPA), where the AB units are connected *via* an amino linker to enable electronic coupling between the chromophores. The chemical structures of both molecules in their all-*E* forms and the parent 4-aminoazobenzene (AAB) as a reference compound are given in Scheme 1.

The influence of chromophore–chromophore interactions and electronic coupling between several addressable AB moieties connected by a central unit on the photoswitching behaviour has rarely been investigated to date. Several studies involve bis-azobenzenes.[34–37] Work by Cisnetti *et al.*[34] on the

[a]*Institut für Physikalische Chemie, Christian-Albrechts-Universität zu Kiel, Olshausenstr. 40, D-24098 Kiel, Germany. E-mail: renth@phc.uni-kiel.de, temps@phc.uni-kiel.de; http://www.uni-kiel.de/phc/temps*
[b]*Institut für Anorganische Chemie, Christian-Albrechts-Universität zu Kiel, Otto-Hahn-Platz 6-7, D-24098 Kiel, Germany*
[c]*Otto Diels-Institut für Organische Chemie, Christian-Albrechts-Universität zu Kiel, Otto-Hahn-Platz 4, D-24098 Kiel, Germany. E-mail: fsoennichsen@oc.uni-kiel.de*

†Electronic supplementary information (ESI) available: Chemical syntheses of BPAPA and TPAPA, X-ray diffraction structure of TPAPA (cif file), tabulated results of excited-state calculations, ^{1}H and 2D-HSQC NMR data for TPAPA. CCDC 897971. For ESI and crystallographic data in CIF or other electronic format see DOI: 10.1039/c2pp25291k

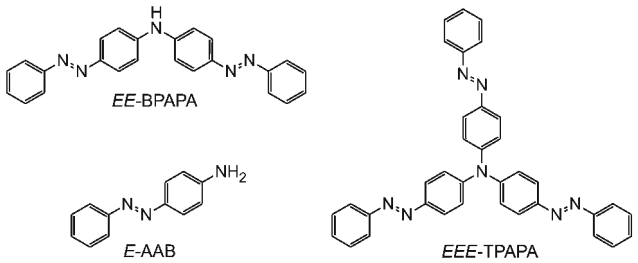

Scheme 1

photo- and electrochemical properties of a *meta*- and a *para*-substituted bis-azobenzene showed a difference in the electronic coupling for the two systems. However, it was not possible to determine the composition in the photostationary states (PSS), which should contain three isomers in both cases. The thermal isomerisation of a conjugated *meta*-substituted bis-azobenzene derivative has been investigated by Robertus *et al.*[37] Both AB units seemed to switch independently of each other, and the thermal behaviour was comparable to that of the single AB derivative. Considering much larger systems, Puntoriero *et al.*[16] determined the photoisomerisation yields of a fourth generation dendrimer containing 32 *trans*-AB units and its complexes with eosin hosted in the dendrimer. Franckevičius *et al.*[18] presented a fluorescence and femtosecond transient absorption study of the excited-state relaxation of dendrimers containing cyano-AB end groups, which indicated rather little effect by the environment. Last but not least, Takahashi *et al.*[30] reported the effect of surface relief grating (SRG) formation by TPAPA. With each AB unit capable of *E*–*Z* isomerisation, this structurally well defined tris-azobenzene may exist in four distinct isomeric forms (*EEE*, *ZEE*, *ZZE*, *ZZZ*). Thus, great potential would arise if the AB units could be individually addressed, a functionality that might be reached by chemical substitutions. Moreover, if TPAPA shows similar hole conductivity as, *e.g.*, the related triphenylamine,[38] it may provide access to logical devices for applications in molecular electronics or to organic light emitting diodes (OLEDs)[39,40] that could be photoswitched to emit at different wavelengths. However, the central question of whether and how the close proximity and electronic interactions of two or more AB moieties in a molecule influence the photoswitching has remained unanswered.

In the present paper, we report on a systematic investigation of the photoswitching properties of the bis- and tris-azobenzenes BPAPA and TPAPA in comparison to the reference compound AAB by means of UV/VIS absorption and NMR spectroscopy. The study is a prelude to subsequent time-resolved dynamics measurements of the molecules. The target compounds were obtained by a modified, less harsh variant of the Ullmann coupling reaction[41,42] between AAB and 4-iodoazobenzene (IAB). To begin with, the nature of the photoexcited electronic states was explored by quantum chemical calculations. The photostationary states for each system were determined by UV/VIS spectroscopy. The relative concentrations and the thermal lifetimes of the individual *EE*-, *EZ*-, *ZZ*-isomers of BPAPA and the *EEE*-, *ZEE*-, *ZZE*-, *ZZZ*-isomers of TPAPA were investigated in acetonitrile solution by conventional ^{1}H NMR and by two-dimensional (2D) HSQC NMR spectroscopy, respectively. The thermal lifetimes of the different isomers are significantly longer for TPAPA compared to BPAPA, which indicates a dependence of the *Z*–*E* isomerisation on the chromophore size and number of AB units. Large differences in the spectral band positions and in the intensities of the absorption spectra of AAB, BPAPA and TPAPA hint at sizable chromophore–chromophore interactions and electronic couplings between the AB moieties.

2. Experimental and computational methods

The protocols for the chemical syntheses of BPAPA and TPAPA are given in the ESI.† All commercially available compounds were purchased from Merck, Sigma-Aldrich, Deutero and Lancaster and used without further purification, except for AAB, which was recrystallised from ethanol. Solvents were dried according to standard procedures. ^{1}H-, ^{13}C-, COSY-, HSQC- and HMBC NMR data were acquired with Bruker AC-200 and Bruker AV-600 spectrometers. UV/VIS absorption spectra were taken on a Shimadzu UV-2401 desktop spectrometer. Three light emitting diodes (Nichia) with emission maxima at λ = 365 nm (NCSU033A, 400 mW), 385 nm (NCSU034A, 400 mW) and 455 nm (NS4C107E, 400 mW) were used for the photoisomerisation experiments. The light intensities were attenuated to 100 mW. The thermal back-isomerisations were followed by UV/VIS and ^{1}H and 2D-HSQC NMR spectroscopies. Quantum chemical calculations of the structures of *EE*-BPAPA and *EEE*-TPAPA in their electronic ground states were performed by density functional theory (DFT) using Gaussian09.[43] AAB had been calculated for another purpose before using the OM2-MRCISD method.[44] The photoexcited electronic states were explored using the second-order approximate coupled-cluster with the resolution-of-the-identity (RI-CC2) model of Turbomole.[45,46]

3. Results

3.1. Molecular structures

The calculated B3LYP/6-31+G(d,p) equilibrium structures of *EE*-BPAPA and *EEE*-TPAPA are displayed in Fig. 1. As can be seen, the molecules adopt propeller-like configurations. The out-of-plane dihedral angles of the AB units in the electronic ground state are ≈21° for BPAPA and ≈42° for TPAPA.

The X-ray diffraction structure of TPAPA (see ESI†) confirmed the calculated propeller-like configuration of the AB units around the central nitrogen. Quite similar configurations are well known for related molecules with a triphenylamine core[47] or triphenylamine itself.[48]

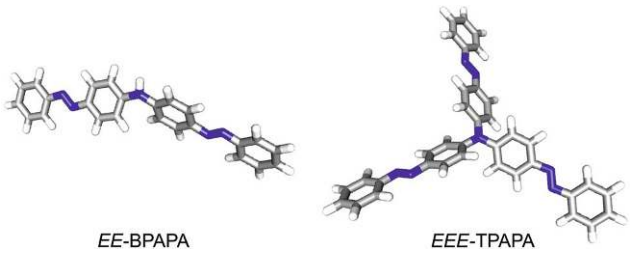

Fig. 1 Calculated structures of *EE*-BPAPA and *EEE*-TPAPA at the B3LYP/6-31+G-(d,p) level of theory.

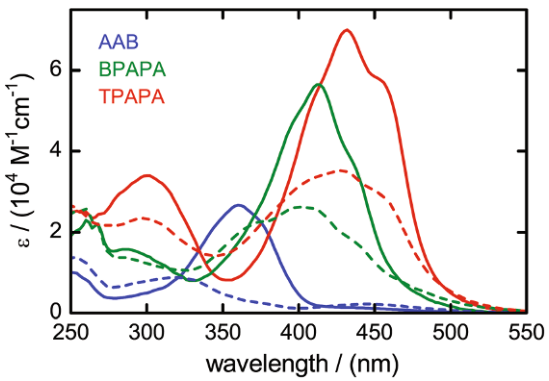

Fig. 2 UV/VIS absorption spectra of *E*-AAB (blue), *EE*-BPAPA (green) and *EEE*-TPAPA (red; solid lines) and in their photostationary states (dashed lines) after irradiation for ≈30 s in the strong first absorption bands at λ = 365 nm (AAB), 385 nm (BPAPA) and 455 nm (TPAPA), respectively, in *n*-hexane (T = 30 °C).

3.2. Stationary UV/VIS absorption spectra

The UV/VIS absorption spectra of AAB, BPAPA and TPAPA in their all-*E* forms in *n*-hexane as the solvent are depicted in Fig. 2. As for unsubstituted AB, AAB shows a strong ππ* band in the near UV with a maximum at λ = 361 nm (ε_{max} = 2.7 × 10^4 M^{-1} cm^{-1}) and a weak nπ* band at $\lambda \approx$ 450 nm in the visible. In contrast, the spectra of BPAPA and TPAPA exhibit pronounced bathochromic and hyperchromic shifts, which increase with the number of AB units. The maxima for BPAPA and TPAPA are at λ = 412 nm (ε_{max} = 5.6 × 10^4 M^{-1} cm^{-1}) and 432 nm (ε_{max} = 7.0 × 10^4 M^{-1} cm^{-1}), respectively. The corresponding nπ* transitions are obscured by the intense ππ* bands, but may be located in the extended wings to the red. The red-shift is more pronounced for BPAPA compared to AAB than for TPAPA compared to BPAPA. Thus, the intramolecular coupling of two (three) AB chromophores in BPAPA (TPAPA) has drastic consequences on the resulting excited electronic states and their energies and spectra.

Also given in Fig. 2 are the absorption spectra of the molecules in the photostationary states PSS365 (AAB), PSS385 (BPAPA) and PSS455 (TPAPA) after irradiation at the specified wavelengths. Similar to unsubstituted AB, where the *Z*-isomer shows a blue-shifted and much weaker ππ* absorption but a stronger nπ* absorption than the *E*-isomer, the spectrum of AAB in the PSS365 exhibits decreased absorption around

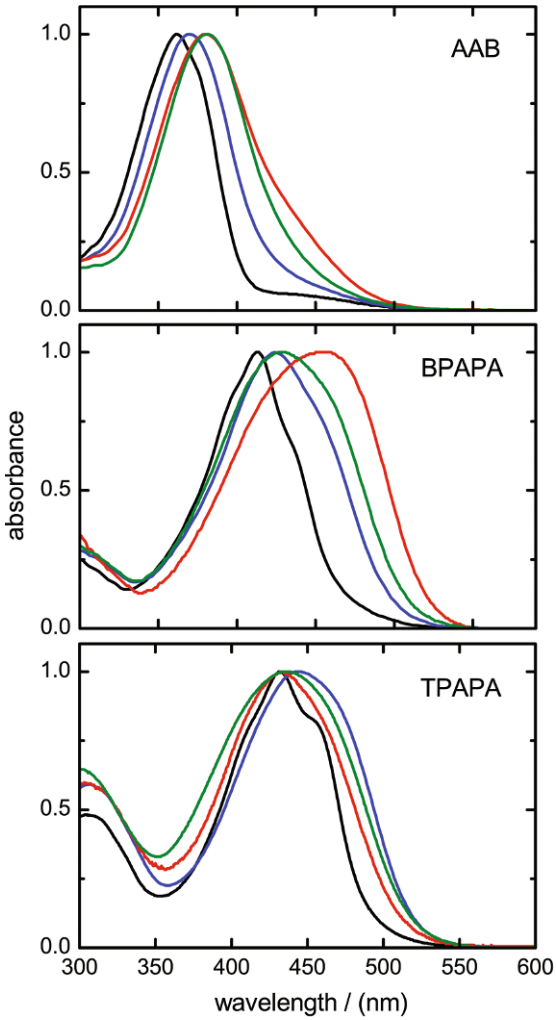

Fig. 3 UV/VIS absorption spectra of AAB (top), BPAPA (middle) and TPAPA (bottom) in *n*-hexane (black), chloroform (blue), acetonitrile (green) and ethanol (red). The absorption maxima were normalized for better comparison.

360 nm compared to the pure *E* isomer and increased absorption around 450 nm. In the PSS385 for BPAPA and PSS455 for TPAPA, the ππ* absorptions are much lower as well. At the same time, the presence of several isomers in both cases results in a significant broadening of the bands. Unfortunately, the lack of clear characteristic spectral signatures of the different isomers in the course of the thermal back-reactions hampers further analysis of the absorption spectra. However, the photoisomerisation yields and isomer-resolved *Z*–*E* back-reactions could be monitored by NMR (below).

Fig. 3 displays the UV/VIS spectra of the molecules in *n*-hexane, chloroform, acetonitrile and ethanol as solvents. The absorption maximum of AAB can be seen to shift from λ_{max} = 361 nm in *n*-hexane to 371 nm in chloroform and 380 nm in acetonitrile and ethanol in line with the increasing solvent polarity. The bands in chloroform, acetonitrile and ethanol are broadened compared to *n*-hexane. Likewise, the absorption maxima of BPAPA are at λ_{max} = 412 nm in *n*-hexane, 424 nm in chloroform, 429 nm in acetonitrile and

455 nm in ethanol. As for AAB, the bathochromic shift is stronger in the more polar solvents. The pronounced red-shift of ≈45 nm in ethanol compared to *n*-hexane can be rationalised by hydrogen bond formation between the solute and solvent. In the case of TPAPA, the influence of the solvent polarity on the absorption behaviour of TPAPA is not as distinctive as for AAB or BPAPA. The absorption maxima are at λ_{max} = 432 nm in *n*-hexane, 444 nm in chloroform and 434 nm in acetonitrile and ethanol. Compared with the very broad and unstructured band shapes in the more polar solvents, the spectra of BPAPA and TPAPA in *n*-hexane show some very weak structure. The variances in the band shifts and shapes may be partly related to the existence of two resp. three transitions in BPAPA and TPAPA and/or to different basicities and polarities of the primary, secondary and tertiary amine.

3.3. Excited-state calculations

The characters of the photoexcited states were studied using the RI-CC2 model[45,46] with the def2-TZVPP basis[49] for AAB and BPAPA and the def2-SVP basis[50] for TPAPA at the aforementioned optimised B3LYP/6-31G+(d,p) structures. The calculations gave the first two excited states of AAB, the first four of BPAPA, and the first six of TPAPA. Table S1 in the ESI† lists the respective excitation energies, oscillator strengths and dominant excited determinants for these states.

The relevant molecular orbitals are displayed in Fig. 4. As can be seen, the energetic order of the states (nπ* < ππ*) remains conserved despite the combination of two resp. three AB units. The first excited state of AAB, the first two of BPAPA and the first three of TPAPA are of nπ* character, while the following ones are of ππ* character. All nπ* states carry very low oscillator strengths from S_0. For BPAPA, the calculated excited states appear in pairs of one with higher and one with lower oscillator strength, as one would expect for an excitonic system. While the two nπ* states (S_1, S_2) are virtually degenerate, the two ππ* states (S_3, S_4) are split by about 0.6 eV. The nπ* states are calculated to have about the same energy as in AAB, while the first ππ* state (S_3) is lowered compared to AAB by about 0.75 eV. Since this state carries the bulk of the oscillator strength, its energetic lowering explains the experimentally observed red-shift of the first strong UV/VIS absorption band of BPAPA relative to AAB. In contrast, the $S_4(\pi\pi^*) \leftarrow S_0$ transition of BPAPA is only rather weakly allowed. The results for TPAPA are not quantitatively comparable to the others because of the smaller basis, but qualitative conclusions can nevertheless be drawn. Similar to BPAPA, the nπ* states (S_1, S_2, S_3) are virtually degenerate, but the n orbitals remain localised on one of the AB units each instead of taking the form of linear combinations delocalised over the molecule. This difference can be rationalized on the grounds of the larger out-of-plane dihedral angles of the AB chromophores. The calculated energies of the ππ* states (S_4, S_5, S_6) are comparable to those of BPAPA. Judged by a comparison to results with the same smaller basis set for BPAPA, the excitation energies for TPAPA obtained with the def2-SVP basis are likely slightly overestimated compared to the expected outcome at higher level (def2-TZVPP). The first two are virtually degenerate and carry large oscillator strengths, the third is calculated to be about 0.65 eV higher in energy and has very low oscillator strength.

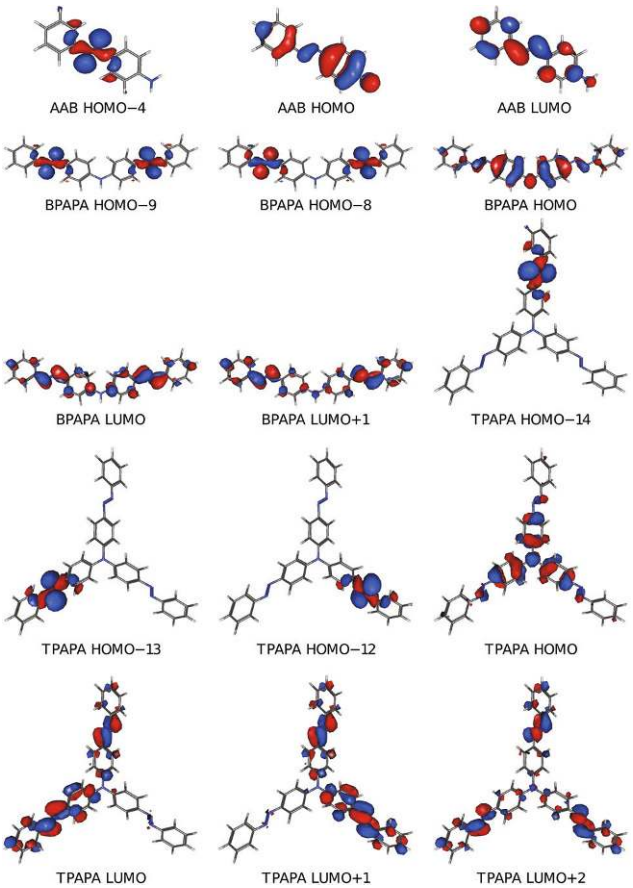

Fig. 4 Relevant molecular orbitals involved in the electronic transitions in the UV/VIS absorption spectra for AAB, BPAPA and TPAPA.

3.4. NMR measurements

The isomer-specific photoisomerisation yields in the photostationary states and the thermal *Z*–*E* back-reactions as a function of time were determined by ^{1}H NMR spectroscopy (BPAPA) and by 2D-HSQC NMR spectroscopy (TPAPA).

Fig. 5 displays ^{1}H NMR spectra of BPAPA in CD_3CN after excitation to the photostationary state PSS385 as a function of time for T = 15 °C. As can be seen, the three singlet peaks of the chemically different NH protons of the three isomers (*EE*, *ZE*, *ZZ*), which co-exist in the PSS, are readily assigned on the basis of their chemical shifts and their time dependence. The NH signal of the *ZZ*-isomer disappears most rapidly, while the NH signal of the *ZE*-isomer shows a slight initial rise due to the *ZE*-production from the *ZZ*-isomer before its subsequent slower decay to zero. The NH signal of the *EE*-isomer slowly rises to its final equilibrium value. All other proton signals can be assigned accordingly (see ESI, section 1.2†). Similar spectra were taken at a slightly elevated temperature (T = 35 °C), where the kinetics were correspondingly faster.

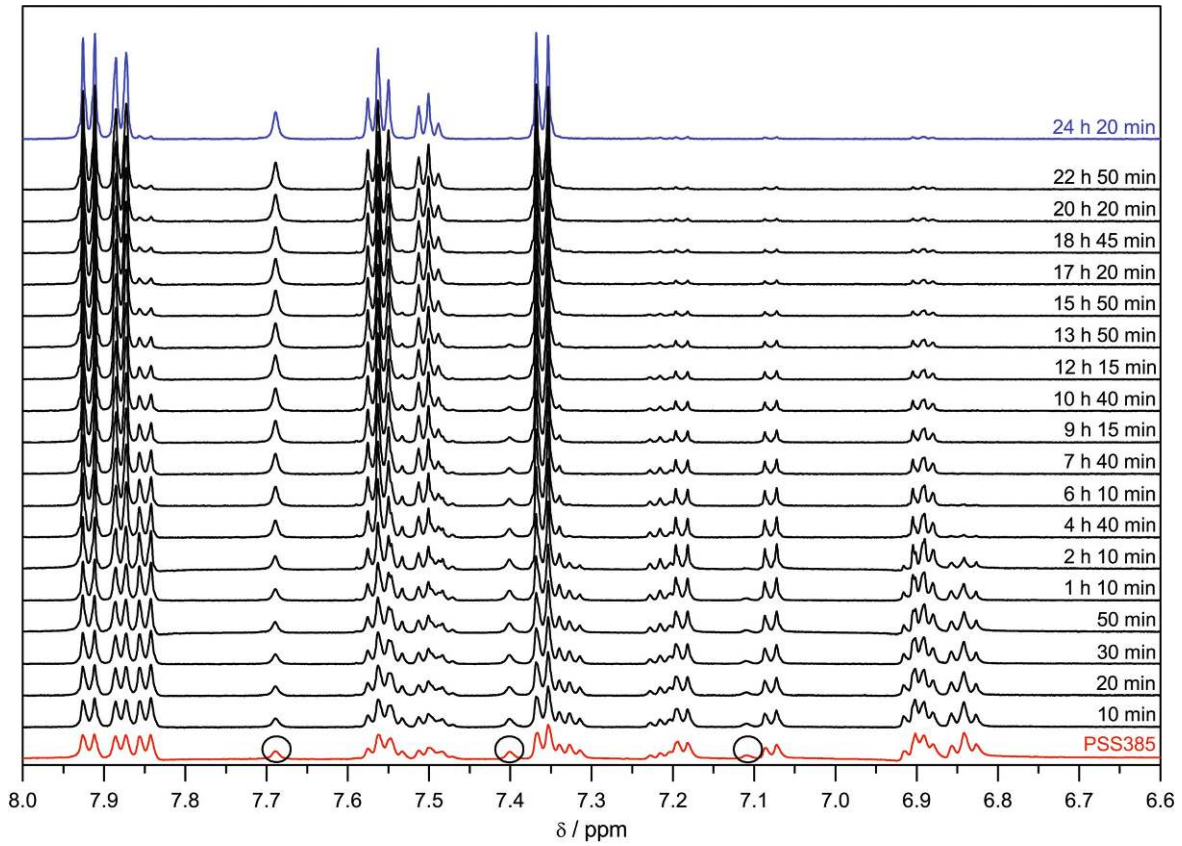

Fig. 5 ^{1}H NMR spectra of BPAPA in CD_3CN at T = 15 °C as a function of time after excitation to the photostationary state PSS385 at t = 0. The circles in the bottom trace highlight the NH proton signals of the three different isomers.

The isomer ratio in the PSS385 was found to be 39% *EE*, 41% *ZE*, and 20% *ZZ*. Taking these data, the isomer-specific thermal lifetimes could be determined by a kinetic analysis of the respective integrated singlet signals for the three NH protons using a consecutive kinetic model including the back-reactions of the *ZZ*- and *EZ*-isomers according to the scheme

$$ZZ \xrightarrow{\tau_{ZZ}} ZE \xrightarrow{\tau_{ZE}} EE$$

The experimental time profiles for the three isomers and the best-fit time profiles for T = 15 °C are shown in Fig. 6. The resulting isomer-specific thermal lifetimes are τ_{ZZ} = 1.9 ± 0.2 h, τ_{ZE} = 7.5 ± 0.6 h (T = 15 °C) and τ_{ZZ} = 0.5 ± 0.1 h, τ_{ZE} = 2.4 ± 0.2 h (T = 35 °C).

Because of the much slower back-reaction compared to BPAPA, similar data for TPAPA were taken only at slightly elevated temperature (T = 35 °C). As for BPAPA, the proton signals belonging to the all-*E* isomer in the spectrum at the longest time are readily recognisable from the time dependence. However, the spectrum of the PSS (see Fig. S1, ESI†) is more congested than in the BPAPA case so that a direct identification of the individual photoisomers was not easily possible. The thermal back-reactions were therefore followed by HSQC NMR spectroscopy to resolve the severe overlap in the ^{1}H NMR spectrum and to assign related cross-peaks to the *EEE*-, *ZEE*-, *ZZE*-, and *ZZZ*-isomers, respectively. The recorded HSQC spectra of the all-*E* isomer, the photostationary state (PSS455), and the photoisomer mixture at three selected times after preparation of the PSS are presented in the ESI (*cf.* Fig. S2†). As shown, the isomer-specific cross-peaks belonging to the aromatic rings next to the central amino-N atom are well separated, the respective concentrations are therefore easily

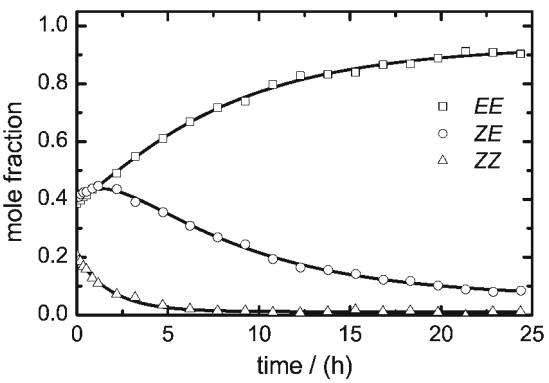

Fig. 6 Time profiles of the *ZZ*-, *ZE*- and *EE*-isomers of BPAPA in the thermal back-reaction starting from the photostationary state PSS385 in CD_3CN at T = 15 °C. The data points (*cf.* Fig. 5) are given by open symbols, the fitted time profiles by solid curves.

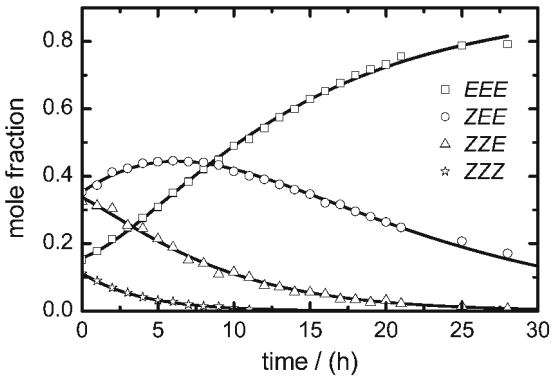

Fig. 7 Time profiles of the *ZZZ*-, *ZZE*-, *ZZE*-, and *ZZZ*-isomers of TPAPA in the thermal back-reaction starting from the photostationary state PSS455 in CD_3CN at T = 35 °C. The data points are given by open symbols, the fitted time profiles by solid curves.

accessible by peak integration. In this way, the photoisomer ratio in the PSS455 was found to be 16% *EEE*, 37% *ZEE*, 36% *ZZE*, and 12% *ZZZ*.

Starting from these values, the respective thermal lifetimes were determined by a kinetic analysis of the time profiles using a consecutive kinetic model including the back-reactions of the *ZZZ*-, *ZZE*-, and *ZEE*-isomers and formation of the *EEE*-isomer of the form

$$ZZZ \xrightarrow{\tau_{ZZZ}} ZZE \xrightarrow{\tau_{ZZE}} ZEE \xrightarrow{\tau_{ZEE}} EEE$$

The experimental time profiles and the fitted curves for the four isomers are given in Fig. 7. The resulting time constants at T = 35 °C for the *ZZZ*-, *ZZE*-, and *ZEE*-isomers are τ_{ZZZ} = 4.0 ± 0.4 h, τ_{ZZE} = 6.4 ± 0.9 h and τ_{ZEE} = 12 ± 1 h, respectively. For reference, the thermal lifetime of the *Z*-isomer of AAB (τ_Z) under similar conditions determined by UV/VIS spectroscopy is of the order of just ≈5 min.

4. Discussion and conclusions

The photoswitching properties of two multi-azobenzene compounds, the secondary amine bis[4-(phenylazo)phenyl]amine (BPAPA) and the tertiary amine tris[4-(phenylazo)phenyl]-amine (TPAPA), have been investigated by means of UV/VIS and NMR spectroscopy in comparison to the primary amine 4-aminoazobenzene (AAB). As expected, the UV/VIS absorption spectra of BPAPA and TPAPA show drastic changes which are understandable on the grounds of the larger π-electron systems by the linkage of two resp. three AB chromophores *via* the central amino-N core, despite the non-coplanar orientation of the AB moieties in the molecules. The observed red-shift of the absorption maximum and the increase in absorbance are more pronounced for BPAPA compared to AAB than for TPAPA compared to BPAPA, which stresses the non-additive effects of the added AB units. This may hint at specific intramolecular interactions, *e.g.*, excitonic coupling or charge-transfer (CT), between the different AB units. It has to be taken into account in addition that the twist angle between the AB units is larger in TPAPA than in BPAPA.

The calculated RI-CC2 excitation energies for the nπ* and the optically bright ππ* excited states of BPAPA and TPAPA are in reasonable agreement with the recorded spectra. The observed strong 412 nm absorption band of BPAPA is attributed to the lower of the two ππ* states, the second ππ* state 0.6 eV higher lacks high oscillator strength. In contrast, the strong 432 nm absorption of TPAPA appears to arise from two degenerate ππ* components with comparable oscillator strengths. The next ππ* state is significantly higher in energy and has only low oscillator strength. The calculated nπ* transitions are very weak, but may contribute to the absorptions in the extended wings in the spectra to the red.

Both BPAPA and TPAPA are efficient photoswitches. Starting from the all-*E* isomers, the prepared photostationary states were found to contain ≈20% all-*Z* isomer in the BPAPA case and ≈12% all-*Z* isomer in the TPAPA case. It should be noted that the transformation of the molecules from the all-*E* to the all-*Z* forms requires two sequential photoisomerisation steps for BPAPA and three such steps for TPAPA. In the photostationary state, a TPAPA molecule on average has nearly 1.5 of its AB units switched to the *Z*-form.

The isomer-specific concentrations in the photostationary states and the thermal back-isomerisation lifetimes for BPAPA and TPAPA were determined by means of ^{1}H NMR and by 2D-HSQC NMR spectroscopy, respectively. In the BPAPA case, the lifetimes with respect to the thermal back-reactions in CD_3CN at T = 35 °C were found to be τ_{ZZ} = 0.5 h and τ_{ZE} = 2.4 h for the *ZZ*- and *ZE*-isomers, respectively. For TPAPA, the corresponding lifetimes at T = 35 °C were found to be τ_{ZZZ} = 4.0 h, τ_{ZZE} = 6.4 h and τ_{ZEE} = 12 h for the *ZZZ*-, *ZZE*-, and *ZEE*-isomers, respectively. The thermal lifetime of *Z*-AAB under similar conditions is only of the order of a few minutes (τ_Z = 5 min). Thus, the *Z*-isomer lifetimes increase considerably with increasing overall chromophore size and number of AB units. This behaviour is related to the changes in the geometric and electronic structures of the molecules, although it cannot be explained unambiguously at the moment.

Towards applications, it is important to understand the intramolecular couplings between the AB units in more detail. Both BPAPA and TPAPA are therefore currently under investigation in our laboratory by femtosecond time-resolved absorption and fluorescence spectroscopy. Ongoing polarisation-dependent decay measurements are expected to provide insight into possible excitonic energy migration processes.

Acknowledgements

The support of this work by the Deutsche Forschungsgemeinschaft through the Sonderforschungsbereich 677 "Function by Switching" is gratefully acknowledged.

References

1 Z. F. Liu, K. Hashimoto and A. Fujishima, Photoelectrochemical information storage using an azobenzene derivative, *Nature*, 1990, **347**, 658–660.

2 T. Ikeda and O. Tsutsumi, Optical switching and image storage by means of azobenzene liquid-crystal films, *Science*, 1995, **268**, 1873–1875.

3 I. Willner and S. Rubin, Control of the structure and functions of biomaterials by light, *Angew. Chem., Int. Ed.*, 1996, **35**, 367–385.

4 H. Rau, Azo compounds, in *Photochromism: Molecules and Systems*, ed. H. Dürr and H. Bouas-Laurent, Elsevier, Amsterdam, 2003.

5 V. Balzani, A. Credi and M. Venturi, *Molecular Devices and Machines: Concepts and Perspectives for the Nanoworld*, Wiley-VCH, Weinheim, 2008.

6 *Molecular Switches*, ed. B. L. Feringa and W. R. Browne, Wiley-VCH, Weinheim, 2011, vol. 1 and 2.

7 T. Hugel, N. B. Holland, A. Cattani, L. Moroder, M. Seitz and H. E. Gaub, Single-molecule optomechanical cycle, *Science*, 2002, **296**, 1103–1106.

8 N. B. Holland, T. Hugel, G. Neuert, A. Cattani-Scholz, C. Renner, D. Oesterhelt, L. Moroder, M. Seitz and H. E. Gaub, Single molecule force spectroscopy of azobenzene polymers: switching elasticity of single photochromic macromolecules, *Macromolecules*, 2003, **36**, 2015–2023.

9 L. Ulysse, J. Cubillos and J. Chmielewski, Photoregulation of cyclic peptide conformation, *J. Am. Chem. Soc.*, 1995, **117**, 8466–8467.

10 O. Pieroni, A. Fissi, N. Angelini and F. Lenci, Photoresponsive polypeptides, *Acc. Chem. Res.*, 2001, **34**, 9–17.

11 S. Spörlein, H. Carstens, H. Satzger, C. Renner, R. Behrendt, L. Moroder, P. Tavan, W. Zinth and J. Wachtveitl, Ultrafast spectroscopy reveals subnanosecond peptide conformational dynamics and validates molecular dynamics simulations, *Proc. Natl. Acad. Sci. U. S. A.*, 2002, **99**, 7998–8002.

12 X. Liang, H. Asanuma and M. Komiyama, Photoregulation of DNA triplex formation by azobenzene, *J. Am. Chem. Soc.*, 2002, **124**, 1877–1883.

13 S. Venkataramani, U. Jana, M. Dommaschk, F. D. Sönnichsen, F. Tuczek and R. Herges, Magnetic bistability of molecules in homogeneous solution at room temperature, *Science*, 2011, **331**, 445–448.

14 A. Archut, F. Vögtle, L. De Cola, G. C. Azzellini, V. Balzani, P. S. Ramanujam and R. H. Berg, Azobenzene-functionalized cascade molecules: photoswitchable supramolecular systems, *Chem.–Eur. J.*, 1998, **4**, 699–706.

15 F. Vögtle, M. Gorka, R. Hesse, P. Ceroni, M. Maestri and V. Balzani, Photochemical and photophysical properties of poly(propylene amine) dendrimers with peripheral naphthalene and azobenzene groups, *Photochem. Photobiol. Sci.*, 2002, **1**, 45–51.

16 F. Puntoriero, P. Ceroni, V. Balzani, G. Bergamini and F. Vögtle, Photoswitchable dendritic hosts: a dendrimer with peripheral azobenzene groups, *J. Am. Chem. Soc.*, 2007, **129**, 10714–10719.

17 R. Deloncle and A.-M. Caminade, Stimuli-responsive dendritic structures: the case of light-driven azobenzene-containing dendrimers and dendrons, *J. Photochem. Photobiol., C*, 2010, **11**, 25–45.

18 M. Franckevičius, R. Vaišnoras, M. Marcos, J. L. Serrano, R. Karpicz and V. Gulbinas, Excited-state relaxation of dendrimers functionalized with cyanoazobenzene-type terminal groups, *Chem. Phys. Lett.*, 2010, **485**, 156–160.

19 V. Chandrasekaran and T. K. Lindhorst, Sweet switches: azobenzene glycoconjugates synthesized by click chemistry, *Chem. Commun.*, 2012, **48**, 7519–7521.

20 J. L. Humphrey, K. M. Lott, M. E. Wright and D. Kuciauskas, Second hyperpolarizability of ethynyl-linked azobenzene molecular wires, *J. Phys. Chem. B*, 2005, **109**, 21496–21498.

21 A. F. Grimes, S. E. Call, E. J. Harbron and D. S. English, Wavelength-resolved studies of Förster energy transfer in azobenzene-modified conjugated polymers: the competing roles of exciton migration and spectral resonance, *J. Phys. Chem. C*, 2007, **111**, 14257–14265.

22 C. Tie, J. C. Gallucci and J. R. Parquette, Helical conformational dynamics and photoisomerism of alternating pyridinedicarboxamide/*m*-(phenylazo)azobenzene oligomers, *J. Am. Chem. Soc.*, 2006, **128**, 1162–1171.

23 E. D. King, P. Tao, T. T. Sanan, C. M. Hadad and J. R. Parquette, Photomodulated chiral induction in helical azobenzene oligomers, *Org. Lett.*, 2008, **10**, 1671–1674.

24 I. Porcar, P. Perrin and C. Tribet, UV-visible light: a novel route to tune the type of an emulsion, *Langmuir*, 2001, **17**, 6905–6909.

25 G. S. Kumar and D. C. Neckers, Photochemistry of azobenzene-containing polymers, *Chem. Rev.*, 1989, **89**, 1915–1925.

26 A. Natansohn and P. Rochon, Photoinduced motions in azo-containing polymers, *Chem. Rev.*, 2002, **102**, 4139–4175.

27 R. Pardo, M. Zayat and D. Levy, Photochromic organic–inorganic hybrid materials, *Chem. Soc. Rev.*, 2011, **40**, 672–687.

28 V. Zaporojtchenko, C. Pakula, S. Wahyuni Basuki, T. Strunskus, D. Zargarani, R. Herges and F. Faupel, Reversible light-induced capacitance switching of azobenzene ether/PMMA blends, *Appl. Phys. A: Solid Surf.*, 2011, **102**, 421–427.

29 M.-J. Kim, E.-M. Seo, D. Vak and D.-Y. Kim, Photodynamic properties of azobenzene molecular film with triphenylamines, *Chem. Mater.*, 2003, **15**, 4021–4027.

30 T. Takahashi, T. Tanino, H. Ando, H. Nakano and Y. Shirota, Surface relief grating formation using a novel azobenzene-based photochromic amorphous molecular material, tris[4-(phenylazo)phenyl]amine, *Mol. Cryst. Liq. Cryst.*, 2005, **430**, 9–14.

31 X. Wang, J. Yin and X. Wang, Photoinduced self-structured surface pattern on a molecular azo glass film: structure–

property relationship and wavelength correlation, *Langmuir*, 2011, **27**, 12666–12676.
32 K. Kreger, P. Wolfer, H. Audorff, L. Kador, N. Stingelin-Stutzmann, P. Smith and H.-W. Schmidt, Stable holographic gratings with small-molecular trisazobenzene derivatives, *J. Am. Chem. Soc.*, 2010, **132**, 509–516.
33 P. Wolfer, H. Audorff, K. Kreger, L. Kador, H.-W. Schmidt, N. Stingelin and P. Smith, Photo-induced molecular alignment of trisazobenzene derivatives, *J. Mater. Chem.*, 2011, **21**, 4339–4345.
34 F. Cisnetti, R. Ballardini, A. Credi, M. T. Gandolfi, S. Masiero, F. Negri, S. Pieraccini and G. P. Spada, Photochemical and electronic properties of conjugated bis(azo) compounds: an experimental and computational study, *Chem.–Eur. J.*, 2004, **10**, 2011–2021.
35 M. V. Peters, R. Goddard and S. Hecht, Synthesis and characterization of azobenzene-confined porphyrins, *J. Org. Chem.*, 2006, **71**, 7846–7849.
36 D. Bléger, J. Dokić, M. V. Peters, L. Grubert, P. Saalfrank and S. Hecht, Electronic decoupling approach to quantitative photoswitching in linear multiazobenzene architectures, *J. Phys. Chem. B*, 2011, **115**, 9930–9940.
37 J. Robertus, S. F. Reker, T. C. Pijper, A. Deuzeman, W. R. Browne and B. L. Feringa, Kinetic analysis of the thermal isomerisation pathways in an asymmetric double azobenzene switch, *Phys. Chem. Chem. Phys.*, 2012, **14**, 4374–4382.
38 S. A. Visser, W. T. Gruenbaum, E. H. Magin and P. M. Borsenberger, Hole transport in arylamine doped polymers, *Chem. Phys.*, 1999, **240**, 197–203.
39 M. Behl, J. Seekamp, S. Zankovych, C. M. Sotomayor Torres, R. Zentel and J. Ahopelto, Towards plastic electronics: patterning semiconducting polymers by nanoimprint lithography, *Adv. Mater.*, 2002, **14**, 588–591.
40 M. Behl, R. Zentel, A. Zen, S. Lucht and D. Neher, Nanostructured polytriarylamines: orientation layers for polyfluorene, *Polym. Mater. Sci. Eng.*, 2004, **90**, 297–298.
41 H. B. Goodbrand and N.-X. Hu, Ligand-accelerated catalysis of the Ullmann condensation: application to hole conducting triarylamines, *J. Org. Chem.*, 1999, **64**, 670–674.
42 A. A. Kelkar, N. M. Patil and R. V. Chaudhari, Copper-catalyzed amination of aryl halides: single-step synthesis of triarylamines, *Tetrahedron Lett.*, 2002, **43**, 7143–7146.
43 M. J. Frisch, G. W. Trucks, H. B. Schlegel, G. E. Scuseria, M. A. Robb, J. R. Cheeseman, G. S. V. Barone, B. Mennucci, G. A. Petersson, H. Nakatsuji, M. Caricato, X. Li, H. P. Hratchian, A. F. Izmaylov, J. Bloino, G. Zheng, J. L. Sonnenberg, M. Hada, M. Ehara, K. Toyota, R. Fukuda, J. Hasegawa, M. Ishida, T. Nakajima, Y. Honda, O. Kitao, H. Nakai, T. Vreven, J. A. Montgomery, J. E. Peralta, F. Ogliaro, M. Bearpark, J. J. Heyd, E. Brothers, K. N. Kudin, V. N. Staroverov, R. Kobayashi, J. Normand, K. Raghavachari, A. Rendell, J. C. Burant, S. S. Iyengar, J. Tomasi, M. Cossi, N. Rega, J. M. Millam, M. Klene, J. E. Knox, J. B. Cross, V. Bakken, C. Adamo, J. Jaramillo, R. Gomperts, R. E. Stratmann, O. Yazyev, A. J. Austin, R. Cammi, C. Pomelli, J. W. Ochterski, R. L. Martin, K. Morokuma, V. G. Zakrzewski, G. A. Voth, P. Salvador, J. J. Dannenberg, S. Dapprich, A. D. Daniels, O. Farkas, J. B. Foresman, J. V. Ortiz, J. Cioslowski and D. J. Fox, *GAUSSIAN09 (Revision A.02)*, Gaussian Inc., Wallingford, CT, U.S.A., 2009.
44 W. Thiel, *MNDO program, version 6.1*, Max-Planck-Institut für Kohlenforschung, Mülheim an der Ruhr, Germany, 2007.
45 C. Hättig and F. Weigend, CC2 excitation energy calculations on large molecules using the resolution of the identity approximation, *J. Chem. Phys.*, 2000, **113**, 5154–5161.
46 C. Hättig, A. Hellweg and A. Köhn, Distributed memory parallel implementation of energies and gradients for second-order Møller–Plesset perturbation theory with the resolution-of-the-identity approximation, *Phys. Chem. Chem. Phys.*, 2006, **8**, 1159–1169.
47 L. Porrès, O. Mongin, C. Katan, M. Charlot, T. Pons, J. Mertz and M. Blanchard-Desce, Enhanced two-photon absorption with novel octupolar propeller-shaped fluorophores derived from triphenylamine, *Org. Lett.*, 2004, **6**, 47–50.
48 G. Meijer, G. Berden, W. L. Meerts, H. E. Hunziker, M. S. de Vries and H. R. Wendt, Spectroscopy on triphenylamine and its van der Waals complexes, *Chem. Phys.*, 1992, **163**, 209–222.
49 F. Weigend, M. Häser, H. Patzelt and R. Ahlrichs, RI-MP2: optimized auxiliary basis sets and demonstration of efficiency, *Chem. Phys. Lett.*, 1998, **294**, 143–152.
50 A. Schäfer, H. Horn and R. Ahlrichs, Fully optimized contracted gaussian basis sets for atoms Li to Kr, *J. Chem. Phys.*, 1992, **97**, 2571–2577.

